Modulation on positions of optical absorption bands in porous Al_2O_3 host/Cr_2O_3

1997 J. Phys.: Condens. Matter 9 6103

(http://iopscience.iop.org/0953-8984/9/28/009)

J. Phys.: Condens. Matter **9** (1997) 6103–6111. Printed in the UK PII: S0953-8984(97)79435-9

Modulation on positions of optical absorption bands in porous Al_2O_3 host/Cr_2O_3

C M Mo†, W L Cai†, G Chen†, X M Li† and L D Zhang‡

† Department of Materials Science and Engineering, University of Science and Technology of China, Hefei 230026, People's Republic of China

‡ Institute of Solid State Physics, Chinese Academy of Sciences, Hefei 230031, People's Republic of China

Received 11 November 1996

Abstract. The optical absorption properties of porous Al_2O_3 host/Cr_2O_3 nanocomposites were investigated. The results show that for each optical reflection spectrum, four absorption bands (p_1–p_4) occur in the wavelength range 200–800 nm. The p_2, p_3 and p_4 bands are induced by the Cr^{3+} $3d^3$ electronic transitions from the $^4A_2$ ground-state energy level to the excited-state energy levels: $^4T_1$, $^4T_2$ and $^4T_2'$ ($^4T_2'$ is formed from splitting of $^4T_2$), respectively. The appearance of p_1 is closely related to the Cr^{3+} and Cr^{4+} ions. For porous Al_2O_3 host/Cr_2O_3 nanocomposites, which are formed by assembling the porous Al_2O_3 host with nano-Cr_2O_3 particles, the positions of absorption bands can be modulated by means of pyrolysis of $Cr(NO_3)_3$ at different temperatures in air, reducing the samples in high purity H_2 and the size confinement of Cr_2O_3 particles by voids in the Al_2O_3 host. With increasing pyrolysis temperature, a blue shift of the absorption bands appears and, inversely, a red shift of the absorption bands takes place when heating the samples in H_2.

1. Introduction

In 1963 McClure [1] reported the polarized optical absorption spectrum of Cr_2O_3 in thin single-crystal plates at room temperature. He observed that three optical absorption bands existed in the wavelength range 300–800 nm. He attributed two absorption bands (p_2 and p_3) located in the range 400–800 nm to the Cr^{3+} $3d^3$ electronic transitions from the $^4A_2$ ground-state level to the excited-state levels, $^4T_1$ and $^4T_2$, respectively. The origin of the optical absorption band (p_1), appearing in the ultraviolet light range, was not explained. Up to now, the optical absorption on nano-Cr_2O_3 has not been reported. In this paper, the characterizations of optical absorption for porous Al_2O_3/Cr_2O_3 nanocomposites were investigated and compared with those of nanostructured Cr_2O_3 bulks of material. The aim of this paper is to modulate the positions of optical absorption bands by means of assembling the porous Al_2O_3 host with nano-Cr_2O_3 particles, pyrolysis at various temperatures in air for $Cr(NO_3)_3$ and reducing the samples in H_2.

2. Sample preparation and experimental studies

Nano-Cr_2O_3 powders with different particle diameters, d, were prepared by pyrolysis of analytically pure $Cr(NO_3)_3 \cdot 9H_2O$ at different temperatures (400, 700, 800, 900, 1000 and 1100 °C, respectively) for 4 h in air. The nanostructured Cr_2O_3 bulks with 13 mm

0953-8984/97/286103+09$19.50

diameter were performed by compacting the powder under a uniaxial pressure of 360 MPa. The porous Al_2O_3 host/Cr_2O_3 nanocomposites were prepared by the following procedure: porous Al_2O_3 host samples were obtained by compacting the powder of α-Al_2O_3 with $d_0 \sim 84$ nm using a uniaxial pressure of 360 MPa and then annealed at 1100 °C for 4 h. After that, they were immersed in a saturated aqueous solution of $Cr(NO_3)_3$ for 1 h. Ions diffused into the water within the pores of Al_2O_3 bulks. After heating at 400, 700, 800, 900, 1000 and 1100 °C, respectively, in air nano-precipitates of Cr_2O_3 were formed in pores.

The x-ray diffraction was carried out on a x-ray diffractometer with CuKα radiation (type D/MAX-rA). All samples were analysed in $10^\circ \leqslant 2\theta \leqslant 80^\circ$ at 100 mA and 40 KV. The phase identification was made by means of JCPDS cards. The average particle diameters of Cr_2O_3 were calculated using Scherrers formula: $d = 0.9\lambda/\beta\cos\theta$, where $\lambda = 0.154$ nm; β (radians) is the width at half height of the diffraction peak, which is induced by the small particle and equals $\beta_m - \beta_0$, where β_m is the measured value of the width of the diffraction peak at half height and β_0 is the width of the diffraction peak at half height caused by the D/MAX-γA diffractometer. $\beta_0 = (\pi/1800)$ rad in $20^\circ \leqslant 2\theta \leqslant 60^\circ$. Therefore, for each x-ray diffraction spectrum six diffraction peaks of Cr_2O_3 in $20^\circ \leqslant 2\theta \leqslant 60^\circ$ are chosen to measure the widths at half height ($\beta_{m1} - \beta_{m6}$). According to Scherrers formula, six d values are calculated, respectively. Then, the arithmetic average values of d_1–d_6 are obtained. The Scherrers formula is an approximate formula. When d is very small, for example, $d \leqslant 25$ nm, the error is about ± 2 nm. When d is in the range 25–60 nm, the error becomes larger, and reaches about ± 5 nm.

Diffuse reflection spectra in the wavelength range 200–800 nm were measured on a visible-ultraviolet spectrophotometer (type Shimadzu UV-240). $BaSO_4$ was used as a reflection reference sample. For all nanostructured Cr_2O_3 bulks and porous Al_2O_3/Cr_2O_3 nanocomposites, before heating in high purity H_2 and after heating at 600 °C in H_2 for 2 h, diffuse reflection spectra were measured.

3. Results

3.1. Phases and particle diameters of Cr_2O_3

Figure 1 shows the evolution of x-ray diffraction spectra for nanostructured Cr_2O_3 bulks (sample 1) (a), porous Al_2O_3/Cr_2O_3 nanocomposites (sample 2) (b), sample 1 after heating in H_2 (c) and sample 2 after heating in H_2 (d), respectively. From figure 1, it can be seen that no phase transformation takes place as the pyrolysis temperature T_p increases. The phase identification indicates that for nanostructured bulks the phase is hexagonal Cr_2O_3 and for porous nanocomposites the phases are the mixture of α-Al_2O_3 and hexagonal Cr_2O_3. Heating nanostructured Cr_2O_3 bulks and porous Al_2O_3/Cr_2O_3 nanocomposites in pure H_2 does not cause phase transformations to take place.

Table 1 gives the particle diameters, d of Cr_2O_3 formed at different pyrolysis temperatures. It is clear that for porous nanocomposites d does not change with increasing T_p, but for nanostructured bulks d increases with the increase of T_p and becomes larger than that of porous nanocomposites.

3.2. Positions of absorption bands

Optical reflection spectra of nanostructured Cr_2O_3 bulks for different pyrolysis temperatures without heating in H_2 and after heating at 600 °C in H_2 for 2 h are shown in figures 2(a) and (b), respectively. It can be seen that four absorption bands (p_1, p_2, p_3 and p_4) occur

Table 1. Phases, particle diameters of Cr_2O_3(d) and peak positions of absorption bands. The positions p_2 and p_3, and the diameters d are in nanometres.

	T_p(°C)														
	400, 4 h			700, 4 h			800, 4 h			900, 4 h			1000, 12 h			1000, 4 h			1100, 4 h		
Samples	d	p_2	p_3	d	p_2	p_3	d	p_2	p_3	d	p_2	p_3	d	p_2	p_3	d	p_2	p_3	d	p_2	p_3
Nanostructured bulks	26		Cr_2O_3	37	460	596 Cr_2O_3	43		Cr_2O_3	48		Cr_2O_3	56		Cr_2O_3	51	460	596 Cr_2O_3	58	460	596 Cr_2O_3
Nanostructured bulks after heating in H_2 for 2 h		464	600 Cr_2O_3	37	464	600 Cr_2O_3							56	464	600 Cr_2O_3				58	464	600 Cr_2O_3
Porous nanocomposites	20		$Cr_2O_3 + Al_2O_3$	20	460	596 $Cr_2O_3 + Al_2O_3$	22	460	596 $Cr_2O_3 + Al_2O_3$	21	456	596 $Cr_2O_3 + Al_2O_3$	23	450	590 $Cr_2O_3 + Al_2O_3$	22	453	590 $Cr_2O_3 + Al_2O_3$	22	450	590 $Cr_2O_3 + Al_2O_3$
Porous nanocomposites after heating in H_2 for 2 h	20		$Cr_2O_3 + Al_2O_3$	20	460	598 $Cr_2O_3 + Al_2O_3$	22	465	600 $Cr_2O_3 + Al_2O_3$	21	460	598 $Cr_2O_3 + Al_2O_3$	21	450	594 $Cr_2O_3 + Al_2O_3$						
Single crystal Cr_2O_3	$p_2 = 471$ nm; $p_3 = 596$–610 nm at room temperature [1]																				

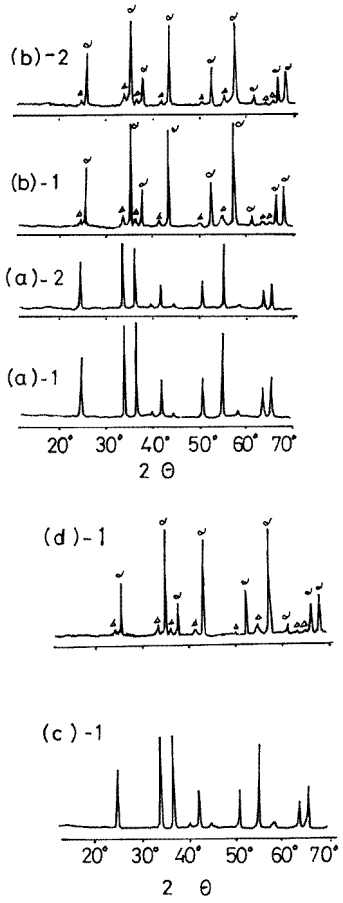

Figure 1. X-ray diffraction spectra of nanostructured Cr_2O_3 bulks (a), porous Al_2O_3/Cr_2O_3 nanocomposites (b), nanostructured Cr_2O_3 bulks after heating in H_2 at 600 °C for 2 h (c) and porous Al_2O_3/Cr_2O_3 nanocomposites after heating at 600 °C in H_2 for 2 h (d). 1, $T_p = 700$ °C; 2, $T_p = 1100$ °C; α, $\alpha - Al_2O_3$; Δ, Cr_2O_3.

in the wavelength range 200–800 nm for each curve. Their peak positions do not change with increasing T_p. The p_1 band is situated in the ultraviolet light range 200–400 nm. The p_2, p_3 and p_4 bands possess peak positions of 460, 596 and ∼710 nm, respectively. From table 1, it can be observed that reducing in H_2 causes the p_2 and p_3 peaks to shift towards the long wavelengths (red shifts) for all nanostructured Cr_2O_3 bulks.

Figure 3 presents the optical reflection spectra of porous Al_2O_3/Cr_2O_3 nanocomposites made by pyrolysis in air without heating in H_2 (a) and after heating at 600 °C in H_2 for 2 h (b), respectively. Curves 1–5 and 7 correspond to T_p of 400, 700, 800, 900, 1000 and 1100 °C for 4 h, respectively. Curve 6 corresponds to 1000 °C for 12 h. Clearly, four absorption bands (p_1–p_4) exist in each curve. In curve 1 the absorption bands become too weak to be observed. Figure 3(a) and table 1 show that by increasing T_p from 700 to 1100 °C, the p_2, p_3 and p_4 bands of porous Al_2O_3/Cr_2O_3 nanocomposites exhibit blue shifts. Namely, their positions shift from 460, 596 and ∼710 nm to 450, 590 and ∼700 nm, respectively. Moreover, the absorption edge at the long-wavelength side of the p_1 band presents a blue shift.

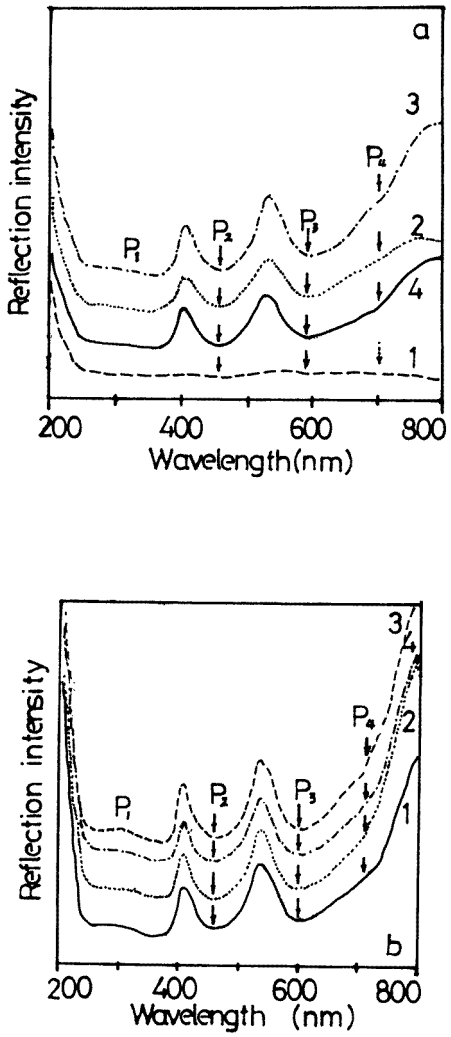

Figure 2. Optical reflection spectra of nanostructured Cr_2O_3 bulks without heating in H_2 (a) and after heating at 600 °C in H_2 for 2 h (b). The arrows show the peak positions (a) Curves 1–4 correspond to a T_p of 400, 700, 1000 and 1100 °C for 4 h, respectively. (b) Curves 1–4 correspond to 400 °C for 4 h, 700 °C for 4 h, 1000 °C for 12 h and 1100 °C for 4 h, respectively.

For porous Al_2O_3/Cr_2O_3 nanocomposites, after heating at 600 °C in H_2 for 2 h, there also exist four absorption bands in each reflection spectrum, as shown in figure 3(b). The peak positions of the p_2 and p_3 bands are listed in table 1. Table 1 demonstrates that: (1) when $T_p \geqslant 900$ °C, the p_2 and p_3 bands of porous Al_2O_3/Cr_2O_3 nanocomposites without heating in H_2 display blue shifts in comparison with those of nanostructured Cr_2O_3 bulks after heating in H_2; (2) for porous nanocomposites after heating at 600 °C in H_2 the p_2 and p_3 bands shift to long wavelengths (red shift) in comparison with those of porous nanocomposites without heating in H_2.

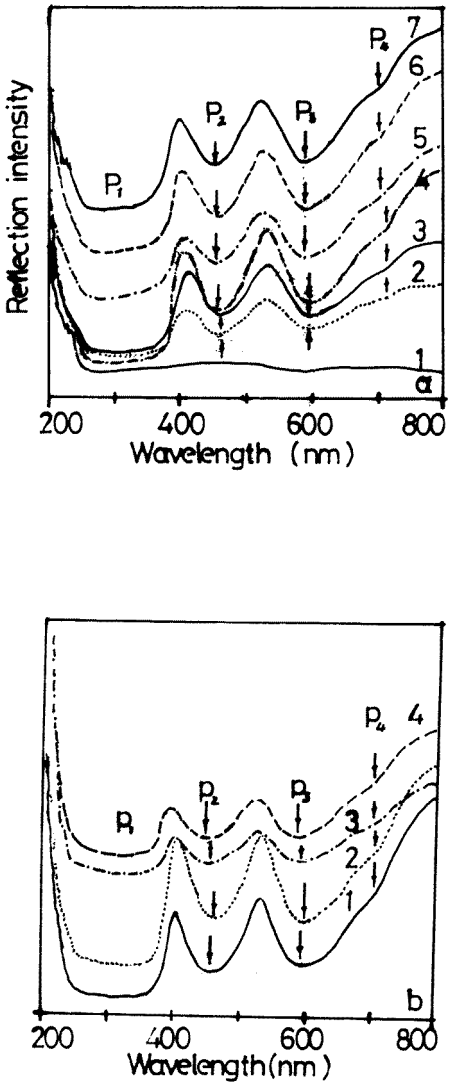

Figure 3. Optical reflection spectra of porous Al_2O_3/Cr_2O_3 nanocomposites without heating in H_2 (a) and after heating at 600 °C in H_2 for 2 h (b). The arrows show the peak positions (a) Curves 1–5 and 7 correspond to the pyrolysis conditions of 400, 700, 800, 900, 1000 and 1100 °C for 4 h, respectively. Curve 6 corresponds to 1000 °C for 12 h. (b) Curves 1–4 correspond to 700 °C for 4 h, 800 °C for 4 h, 900 °C for 4 h and 1000 °C for 12 h, respectively.

4. Discussion

4.1. Mechanisms of nano-Cr_2O_3 absorption bands

McClure [1] observed three optical absorption bands (p_1–p_3) in the wavelength range 350–800 nm at room temperature for Cr_2O_3 single crystal. He attributed the p_2 and p_3 peaks to Cr^{3+} $3d^3$ electronic transitions from the ground-state energy level $^4A_2$ to the excited-state energy levels $^4T_1$ and $^4T_2$, respectively. Moreover, he pointed out that strain inside the

Cr_2O_3 crystal led to the $^4T_2$ peak splitting into two peaks because the $^4T_2$ energy level was split into two energy levels. For nanostructured Cr_2O_3 bulks and porous Al_2O_3/Cr_2O_3 nanocomposites, four absorption bands appear in the wavelength range 200–800 nm (p_1–p_4) at room temperature and the positions of p_2 and p_3 shift to the shorter wavelengths in comparison with those of Cr_2O_3 single crystals (see table 1). Therefore, the p_2 and p_3 bands for nanostructured Cr_2O_3 bulks and porous Al_2O_3/Cr_2O_3 nanocomposites can be attributed to the Cr^{3+} $3d^3$ electronic transitions from $^4A_2$ to $^4T_1$ and $^4T_2$, respectively. Since nano-Cr_2O_3 may be nonstoichiometric, in other words, more oxygen vacancies exist in each nano-Cr_2O_3 particle, resulting in severe distorsions of the O^{2-} octahedrons around Cr^{3+}. This distorsion causes the $^4T_2$ energy level to be split into two energy levels. Therefore, the $^4T_2$ peak is split into two peaks (p_3 and p_4).

The p_1 band is located in the ultraviolet range. Hommerich *et al* [2] indicated that the Cr^{4+} and Cr^{6+} ions could induce strong ultraviolet absorption. Hou *et al* [3] reported that there existed about 1% CrO_2 in Cr_2O_3 formed by pyrolysis of $Cr(NO_3)_3$. Therefore, it can be supposed that the p_1 band in our experiments is closely related to the Cr^{4+} ions. This does not imply, however, that the p_1 band is mainly caused by the Cr^{4+} ions. From figures 3(a) and (b), it is clear that when the pyrolysis temperature is 700 or 800 °C, the p_1 band of porous Al_2O_3/Cr_2O_3 nanocomposites after heating in H_2 becomes obviously strong in comparison with that of porous Al_2O_3/Cr_2O_3 nanocomposites without heating in H_2. As we know, reducing in H_2 probably causes Cr^{4+} to change into Cr^{3+}. If the p_1 band is induced only by the Cr^{4+} ions, the p_1 band for samples after reducing in H_2 should decrease. Therefore, the intensity increase of the p_1 band suggests that the p_1 band cannot be attributed only to the Cr^{4+} ions and thus it is possible that the p_1 band is associated with both the Cr^{4+} and Cr^{3+} ions.

4.2. Movement of peak positions of absorption bands

With increasing T_p all absorption bands of porous Al_2O_3/Cr_2O_3 nanocomposites exhibit blue shifts (see figure 3(a) and table 1), but for nanostructured Cr_2O_3 bulks all bands do not move (see figure 2(a) and table 1). As we know, the position of each absorption band is mainly determined by the blue shift effect and the red shift effect. Before formation of nanostructured Cr_2O_3 bulks, the Cr_2O_3 powder was obtained by pyrolysis of $Cr(NO_3)_3$ in air at different temperatures. As a result, there are quite rare oxygen vacancies in Cr_2O_3 particles, because during pyrolysis enough oxygen in air is provided to form Cr_2O_3. In other words, the number of oxygen vacancies in nanostructured bulks decreases slightly with the increasing T_p. This will cause the red shift effect of the absorption band to decrease. This can be explained as follows. As we know, with decreasing D_q/B (D_q is the crystal-field strength and B is the crystal-field parameter), the spacing between the $^4A_2$ level and the $^4T_1$ level becomes smaller [5]. The existence of oxygen vacancies makes the average distance between Cr^{3+} and O^{2-} ions (R) increase; the more the oxygen vacancies, the larger R. D_q is directly proportional to r^4/R^5, where r is the average radius of the Cr^{3+} $3d^3$ electronic orbit. Therefore, the increase of oxygen vacancies leads D_q to decrease. B depends on the repulsive action between electrons; the larger the repulsion, the higher the B value. The elevation of oxygen vacancies leads R to increase and the O^{2-} 2p electrons to decrease, so that the average coupling effect between Cr^{3+} 3d and O^{2-} 2p electrons becomes weak and the average screening effect of O^{2-} 2p electrons to Cr^{3+} 3d electrons descends. This induces the repulsive action between Cr^{3+} 3d electrons to be enhanced, resulting in the ascension of the average repulsion between electrons. Therefore, B ascends with increasing oxygen vacancies.

According to the above discussion, the following conclusion can be obtained. With the increase of oxygen vacancies, D_q/B decreases and, hence, the spacing between $^4A_2$ and $^4T_2$ (and $^4T_1$) descends. This will cause the red shift of the absorption bands to increase. Inversely, the decrease of the oxygen vacancies gives rise to the red shift effect to drop. This is why the red shift effect decreases with the increase of T_p.

In addition, when T_p increases from 700 to 1100 °C, d changes from 37 to 58 nm. This makes the blue shift effect weaken. Since Cr_2O_3 possesses a semiconductor character, the absorption spectrum of semiconductor nanocrystals is usually blue shifted relative to the bulk sample [6–9]. The blue shift is attributed to the molecular character of the wavefunction in the small particles. The atomic wavefunction overlap is smaller and the bands are flatter and narrower in the small particles than in the large ones and the bulk [4]. This implies that when decreasing the diameter of the particle, the spacing between the energy levels becomes larger. As a result, the absorption band, which arises from the electronic transitions from the lower energy level to the higher energy level, exhibits a blue shift. This is why the blue shift effect becomes weak with increasing T_p when the Cr_2O_3 particle diameter increases.

In summary, with raising T_p, both the red shift effect and the blue shift effect become weak. Therefore, for each T_p the influences of blue shift and red shift cancel out each other. This is why the absorption bands of nanostructured bulks do not move with increasing T_p.

For porous Al_2O_3/Cr_2O_3 nanocomposites, however, the Cr_2O_3 particles are formed in voids of the Al_2O_3 host by pyrolysis of $Cr(NO_3)_3$. In voids there is not sufficient oxygen for Cr_2O_3 to form, resulting in an absence of oxygen in Cr_2O_3 particles. This causes the fact that in Cr_2O_3 particles more oxygen vacancies exist than in the nanostructured Cr_2O_3 bulks; the higher the pyrolysis temperature, the fewer the oxygen vacancies. This causes the red shift to decrease with increasing T_p. The blue shift effect does not change with T_p, however, because the particles do not grow with T_p owing to the confinement of voids (see table 1). Therefore, all absorption bands of porous Al_2O_3/Cr_2O_3 nanocomposites present a blue shift with increasing T_p.

After heating in H_2, in most cases, the absorption bands (p_2–p_4) of porous Al_2O_3/Cr_2O_3 nanocomposites show red shifts in comparison with those of porous Al_2O_3/Cr_2O_3 nanocomposites without heating in H_2 (see figure 3 and table 1). For nanostructured Cr_2O_3 bulks after heating in H_2 the red-shift phenomenon is also observed (see figure 2 and table 1). This red-shift phenomenon is attributed to the increase of the number of oxygen vacancies induced by reducing in H_2.

5. Conclusions

(1) In the wavelength range 200–800 nm four optical absorption bands (p_1–p_4) exist for each reflection spectrum of nanostructured Cr_2O_3 bulks and porous Al_2O_3/Cr_2O_3 nanocomposites. The p_2, p_3 and p_4 peaks are induced by the Cr^{3+} $3d^3$ electronic transitions from the ground-state energy level, $^4A_2$, to the excited-state energy levels, $^4T_1$, $^4T_2$ and $^4T_2'$, which is formed from splitting of $^4T_2$, respectively, and the p_1 band is closely associated with both the Cr^{3+} and Cr^{4+} ions.

(2) For nanostructured Cr_2O_3 bulks only red shifts of the absorption bands can be realized by heating the sample in highly pure H_2, while for porous Al_2O_3/Cr_2O_3 nanocomposites the positions of the absorption bands can be modulated. Thus, red shifts and blue shifts of the absorption bands are realized by heating the porous nanocomposites in H_2 and by increasing the pyrolysis temperature of $Cr(NO_3)_3$ in voids of the porous Al_2O_3 host when preparing porous Al_2O_3 host/Cr_2O_3 nanocomposites.

Acknowledgments

This project is supported by the Climbing Program, Key project of National Fundamental Research and Natural Science Foundation of China.

References

[1] McClure D S 1963 *J. Chem. Phys.* **38** 2289
[2] Hommerich U, Eilers H, Yen W M, Hayden J S and Aston M K 1994 *J. Luminescence* **60&61** 119
[3] Hou B, Ji X, Xie Y, Li J, Shen B and Qian Y 1995 *Nanostruct. Mater.* **5** 529
[4] Vassiliou J K, Mehrotra V, Russell M W, Giannelis E P, McMichael R D, Shull R D and Ziolo R F 1993 *J. Appl. Phys.* **73** 5109
[5] Weber M J 1981 Laser excited fluorescence spectroscopy in glass *Laser Spectroscopy of Solids* vol 49 ed W M Yen and P M Selzer (Berlin: Springer)
[6] Fauchet P M, Tsai C C and Tanaka K (eds) 1990 *Materials Issues in Microcrystalline Semiconductors* (Pittsburgh, PA: Materials Research Society)
[7] Smith D K and Mailhiot C 1990 *Rev. Mod. Phys.* **62** 173
[8] Merkt U and Sikorski C 1990 *Semicond. Sci. Technol.* **5** S182
[9] Ramakrichna M V and Friesner R A 1991 *Phys. Rev. Lett.* **67** 629